

Towards lifelong learning of Recurrent Neural Networks for control design

Fabio Bonassi^{1,*}, Jing Xie¹, Marcello Farina¹, and Riccardo Scattolini¹

Abstract—This paper proposes a method for lifelong learning of Recurrent Neural Networks, such as NNARX, ESN, LSTM, and GRU, to be used as plant models in control system synthesis. The problem is significant because in many practical applications it is required to adapt the model when new information is available and/or the system undergoes changes, without the need to store an increasing amount of data as time proceeds. Indeed, in this context, many problems arise, such as the well known Catastrophic Forgetting and Capacity Saturation ones. We propose an adaptation algorithm inspired by Moving Horizon Estimators, deriving conditions for its convergence. The described method is applied to a simulated chemical plant, already adopted as a challenging benchmark in the existing literature. The main results achieved are discussed.

Index Terms—Recurrent Neural Networks, adaptation, machine learning, lifelong learning, control design.

I. INTRODUCTION

Nowadays, one of the most up-to-date topics in Machine Learning (ML) research is the so-called *lifelong learning*, see for instance the recent reviews [1], [2], [3], [4]. The formulation of the problem, also called *incremental learning* [5], [6], *never-ending learning* [7], or *continual learning* [1], is quite intuitive. Assume that a Machine Learning method is used to retrieve a model of a dynamical system, by means of suitable training and validation procedures. Then, provided that new data are available, how and when should this model be updated, i.e. re-tuned?

The lifelong learning problem is particularly relevant when such a model is used to synthesize a model-based control law. Indeed, even if the adopted control strategy guarantees closed-loop stability and robustness properties in the nominal case, should the plant exhibit time-varying characteristics, adaptation would typically be required to preserve the stability characteristics as well as to maintain performance throughout the plant life-span. In this framework, two main cases of adaptation can be considered.

Case 1: Over time, new data are collected, either under the same operating conditions as the data previously used for model training and testing, or at least under conditions of plant parameters slowly varying over time. These new data can be thus used to improve the model accuracy.

Case 2: the plant moves to new and unexplored operating conditions. That is, the data generation system significantly changes over time, and the existing model is unable to represent the new system behavior.

* Corresponding author

¹ The authors are with the Dipartimento di Elettronica, Informazione e Bioingegneria, Politecnico di Milano, Via Ponzio 34/5, 20133, Milano, Italy. E-mail: name.surname@polimi.it

In order to face these cases, various life-learning ML techniques have been proposed to guarantee properly tuned and frequently updated models, without the need to store and process an increasingly larger amount of data. Indeed, to deal with *Case 1*, the obvious idea is to re-tune the model parameters based on the new available data, while for *Case 2* it can be more advisable to enlarge the model structure, so as to improve the model capability to represent different operating conditions, which generally implies the necessity to re-train the model from scratch.

Both these approaches have, however, their own drawbacks. Namely, concerning *Case 1*, re-tuning the model when new data are available can lead to the so-called *Catastrophic Forgetting* problem, which happens when the knowledge previously embedded in the model is discarded by the re-tuning procedure itself, with consequent reduced description capabilities, see [4].

As for *Case 2*, selecting new model structures generally leads to a model which is unable of retaining the previous representation capabilities, let alone of well describing the new operating conditions. This phenomenon is usually named *Capacity Saturation*, see again [4], and is especially found in many machine-learning models, for which a change in structure implies the need to repeat the entire training procedure.

Among the established models for dynamical systems control design, Neural Networks (NNs), and in particular Recurrent Neural Networks (RNNs). They owe their wide popularity in the control community to their ability to resemble dynamic models that can be proficiently used to design model-based control strategies, such as Model Predictive Control (MPC). In this context, a popular family of RNN is the one of Neural Nonlinear AutoRegressive eXogenous (NNARX) networks, see [8], [9], [10], [11], [12], and [13], [14], [15] for the joint use of NNARX models and MPC. One of the main advantages of NNARXs is that their state correspond to past inputs and outputs, so that observers are not required to implement a state-feedback control law. A second family of RNNs, characterized by a simple structure particularly easy to tune, is the one of Echo State Networks (ESNs), originally introduced in [16], and subsequently used for control design in [17], [18]. However, in view of their excellent performance in a wide class of problems, the most popular RNN are the Long Short Term Memory (LSTM) networks [19], [20]. Finally, Gated Recurrent Units (GRU) [21], [22], although characterized by a simpler structure than LSTMs, have been shown to achieve satisfactory performances in a number of applications [23], and they are hence considered as a valuable, yet simpler, alternative to LSTMs.

Theoretical foundations for the use of NNARX, ESN, LSTM, and GRU for system identification and control have recently been laid in terms of Input-to-State Stability (ISS) [24], [25] and Incremental Input-to-State-Stability (δ ISS) [26], [27], see [28], [29], [30], [31], [32]. These stability notions have then been leveraged when using these networks for MPC design, see [32], [33].

In this context, the aim of this paper is to draw a research line for a possible solution to the lifelong learning for the previously described RNN architectures. Specifically, *Case 1* is considered, i.e. a model of the plant with constant or slowly-varying parameters. To this end, we propose an approach based on the Moving Horizon Estimation (MHE), an optimization-based strategy which has been widely investigated and used by the control community, see [34], [35]. In particular, the proposed method relies on the algorithm described in [36] – suitably extended to cope with the specific problem at hand – to tune the weights of the RNN model so as to improve its modeling performances.

This strategy is quite different from the solutions currently adopted by the machine learning community, which consist of ad-hoc NN structures and learning algorithms, see e.g. [37], [38], [39]. Such strategies may indeed be well-suited to *Case 2*, where new operating regions are progressively explored by the system, at the price of significantly complicating the control design stage.

The paper is organized as follows. In Section II the problem is stated, and the proposed algorithm for the periodic tuning and adaptation of the RNN is described. Section III is devoted to present the application of the proposed method to a nontrivial simulation example, consisting of a nonlinear plant made by two chemical reactors and one separator. The example, taken from [40], is characterized by a strongly nonlinear behavior, and it is believed to represent a challenging benchmark for the class of problems here considered. Finally, Section IV closes the paper with some conclusions and hints for future works.

II. PROBLEM FORMULATION AND ADAPTATION ALGORITHM

Consider a RNN model, belonging to one of the families NNARX, ESN, LSTM, or GRU, which can be described as a dynamical system in the following generic form [32]:

$$\begin{cases} x_{k+1} = f(x_k, u_k; \Theta) \\ y_k = g(x_k, u_k; \Theta) \end{cases}, \quad (1)$$

where k is the discrete time index, Θ is the vector of network’s parameters, called weights, and x , u , y are the state, input, and output vectors, respectively. The input u is assumed to lie in a compact set \mathcal{U} containing the origin. In addition, it is assumed for simplicity that the state x is available; note that this is always true for NNARXs.

We herein assume that the real plant to be estimated is fully described by (1) with $\Theta = \Theta^o$, where of course Θ^o is unknown and unique. In other words, we assume that no measurement noise affects the system, and that the structure

of the NN model coincides with that of the plant, though its parameters must be properly tuned. To this end, the algorithm described in the following, based on MHE, is proposed.

A. RNN parameters’ update algorithm for lifelong learning

The proposed algorithm is intended to be run periodically every N steps, where N is a positive integer corresponding to the length of the time-window throughout which the data is collected from the system. Thus, at $k = tN$, with $t \in \{1, 2, \dots\}$, an optimization problem is formulated, which seeks the parameters update that best explains the collected data. In this setting, the model weights constitute an optimization variable, denoted by Θ_k . The underlying MHE optimization problem at $k = tN$ can be stated as

$$\begin{aligned} \Theta_k^* = \arg \min_{\Theta_k} \left\{ J_k(\Theta_k) = \sum_{i=0}^N \|y_{k-i} - \hat{y}_{k-i}\|^2 + \right. \\ \left. + \mu \|\Theta_k - \Theta_{k-N}^*\|^2 \right\} \\ \text{s.t. } \hat{x}_{k-N} = x_{k-N} \\ \hat{x}_{k-i} = f(\hat{x}_{k-i-1}, u_{k-i-1}; \Theta_k) \\ \hat{y}_{k-i} = g(\hat{x}_{k-i-1}, u_{k-i-1}; \Theta_k) \\ \forall i \in \{0, \dots, N\} \end{aligned} \quad (2)$$

where Θ_{k-N}^* denotes the optimal solution to (2) at time $k-N$. Note that the cost function J_k penalizes the mismatch between the past measured output y_{k-i} , with $i \in \{0, \dots, N\}$, and that of the NN model, i.e. \hat{y}_{k-i} , obtained initializing (1) in x_{k-N} and simulating it with the same input applied to the plant. The second term of J_k discourages significant deviations from the previously computed optimal solution Θ_{k-N}^* . Hence, the coefficient μ defines the trade-off between the need to improve the model’s performances (μ “small”), and the necessity not to forget the information previously acquired, i.e. to avoid the catastrophic forgetting. In this sense, Θ_{k-N}^* can be regarded as a prior for the optimization procedure at time tN . The optimal solution Θ_k^* represents the updated set of weight of the model (1). At time $k = (t+1)N$ the optimization procedure is then repeated.

B. Convergence properties

Under the stated assumptions, the properties of the proposed MHE algorithm can now be proved along the lines of [36]. To this end, let us define the function γ_{-i} as the one that relates, for all $i \in \{0, \dots, N\}$, the output y_{k-i} to the initial state x_{k-N} and to the sequence of previous inputs, denoted by $\mathbf{u}_{k-i} = \{u_{k-N}, \dots, u_{k-i}\}$. These functions can hence be defined as the concatenation of the system’s equations (1)

$$y_{k-i} = \gamma_{-i}(x_{k-N}, \mathbf{u}_{k-i}; \Theta^o), \quad (3)$$

$$\hat{y}_{k-i} = \gamma_{-i}(x_{k-N}, \mathbf{u}_{k-i}; \Theta_k). \quad (4)$$

It is hence possible to define the vector of output reconstruction errors as

$$\Gamma_k(\Theta^o, \Theta_k) = \begin{bmatrix} \gamma_{-N}(x_{k-N}, \mathbf{u}_{k-N}; \Theta^o) - \gamma_{-N}(x_{k-N}, \mathbf{u}_{k-N}; \Theta_k) \\ \vdots \\ \gamma_{-1}(x_{k-N}, \mathbf{u}_{k-1}; \Theta^o) - \gamma_{-1}(x_{k-N}, \mathbf{u}_{k-1}; \Theta_k) \\ \gamma_0(x_{k-N}, \mathbf{u}_k; \Theta^o) - \gamma_0(x_{k-N}, \mathbf{u}_k; \Theta_k) \end{bmatrix}. \quad (5)$$

We introduce the following assumption:

Assumption 1: There exist a K -function φ such that

$$\|\Gamma_k(\Theta^o, \Theta_k)\|^2 \geq \varphi(\|\Theta^o - \Theta_k\|^2) \quad (6)$$

and a positive scalar δ such that, for any Θ^o and Θ_k ,

$$\frac{\varphi(\|\Theta^o - \Theta_k\|^2)}{\|\Theta^o - \Theta_k\|^2} \geq \delta. \quad (7)$$

Letting

$$\varepsilon_k = \|\Theta^o - \Theta_k^*\|^2,$$

the main result can be stated.

Proposition 1: If

$$\frac{2\mu}{\frac{1}{2}\mu + \delta} < 1 \quad (8)$$

then $\varepsilon_k \rightarrow 0$ as $k \rightarrow \infty$.

Proof: Along the lines of [36], let us first compute an upper bound of the cost function J_k defined in (2), evaluated at the optimal value of the parameters Θ_k^* . To this end, consider $J_k(\Theta^o)$, and note that in this case $\|y_{k-i} - \hat{y}_{k-i}\|^2 = 0$, for all $i = 0, \dots, N$, since the model matches the plant. This implies that

$$J_k(\Theta^o) = \mu \|\Theta^o - \Theta_{k-N}^*\|^2 = \mu \varepsilon_{k-N}. \quad (9)$$

Then, in view of the optimality of Θ_k^* , one has that

$$J_k(\Theta_k^*) \leq J_k(\Theta^o) = \mu \varepsilon_{k-N}. \quad (10)$$

At this stage, let us recall that, by standard norm arguments, for any vector z_a, z_b, \bar{z} it holds that

$$\begin{aligned} \|z_a - z_b\|^2 &\leq \|z_a - \bar{z}\|^2 + \|z_b - \bar{z}\|^2 + 2\|(z_a - \bar{z})(z_b - \bar{z})\| \\ &\leq \|z_a - \bar{z}\|^2 + \|z_b - \bar{z}\|^2 + \|z_a - \bar{z}\|^2 + \|z_b - \bar{z}\|^2 \\ &\leq 2\|z_a - \bar{z}\|^2 + 2\|z_b - \bar{z}\|^2, \end{aligned} \quad (11)$$

where Young's inequality has been applied with $p = q = 1$. Thus, from (11) it follows that

$$\|z_a - \bar{z}\|^2 \geq \frac{1}{2}\|z_a - z_b\|^2 - \|\bar{z} - z_b\|^2. \quad (12)$$

This inequality can be used to retrieve a bound of $J_k(\Theta_k^*)$. Taking Θ_k^* , Θ_{k-N}^* , and Θ^o as z_a , \bar{z} , and z_b , respectively, the second term of $J_k(\Theta_k^*)$ can be bounded as:

$$\begin{aligned} \mu \|\Theta_k^* - \Theta_{k-N}^*\|^2 &\geq \frac{\mu}{2} \|\Theta_k^* - \Theta^o\|^2 - \mu \|\Theta_{k-N}^* - \Theta^o\|^2 \\ &= \frac{1}{2} \mu \varepsilon_k - \mu \varepsilon_{k-N} \end{aligned} \quad (13)$$

The first term of $J_k(\Theta_k^*)$, i.e. $\sum_{i=0}^N \|y_{k-i} - \hat{y}_{k-i}\|^2$, by definition can be expressed as $\|\Gamma_k(\Theta^o, \Theta_k^*)\|^2$. Hence, in light of (7), $J_k(\Theta_k^*)$ satisfies

$$J_k(\Theta_k^*) \geq \frac{1}{2} \mu \varepsilon_k - \mu \varepsilon_{k-N} + \delta \varepsilon_k \quad (14)$$

By combining (10) and (14), we finally have that the dynamics of the the error ε is governed by

$$\varepsilon_k \leq \frac{2\mu}{\frac{1}{2}\mu + \delta} \varepsilon_{k-N}. \quad (15)$$

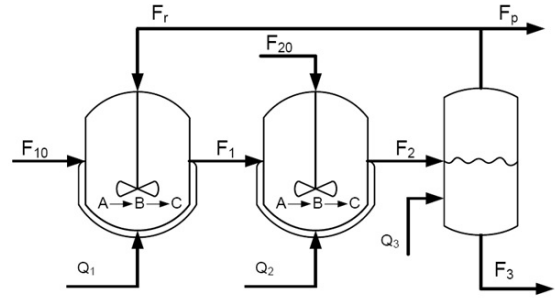


Fig. 1. Schematic of the considered chemical benchmark plant.

Thus, if (8) holds, the error converges. \blacksquare

It is worth noticing that condition (8) can always be satisfied provided that the tuning parameter μ is chosen sufficiently small, i.e. $\mu < \frac{2}{3}\delta$. However, too small values of μ can lead the value of Θ^* to depend, to a large extent, on the most recent data (and possibly on noise), and ultimately leading to Catastrophic Forgetting, so that a suitable trade-off must be suitably selected.

Remark 1: In the formulation of the adaptive algorithm described above, two fundamental assumptions have been implicitly introduced. The first one is that there exist a unique unknown parametrization Θ^o for which the RNN model perfectly describes the plant's dynamics. Secondly, it has been assumed that the plants' parameters are constant, i.e. Θ^o is fixed. However, the most natural framework to use the described method is the one where there is a plant/model mismatch, and the plant parameters are (very) slowly varying. While for this setting the proposed theoretical results are not guaranteed to hold, the tests performed on the numerical example discussed in Section III show that these assumptions can in practice be relaxed.

III. SIMULATION EXAMPLE

To test the proposed strategy on a realistic problem, we applied the lifelong learning approach discussed in Section II to an LSTM network describing the dynamics of the chemical benchmark system depicted in Figure 1, which has been previously considered in [40] and [41] as a challenging problem for control design and estimation.

A. Chemical benchmark system description

The chemical plant is composed of two reactors and one separator. The reactant liquid A feeds the two reactors, where it is converted into the products B and C. There is also a recirculation flow from the separator to the first reactor that makes the system strongly coupled. The physical model of the plant is composed of twelve nonlinear continuous-time differential state equations, describing mass and energy balances. These equations determine, for each reactor ($i = 1$ and $i = 2$) and for the separator ($i = 3$), the dynamics of the liquid's level H_i , its temperature T_i , and the concentrations of chemical products A and B, denoted by x_{Ai} and x_{Bi} ,

TABLE I
PARAMETERS OF THE CHEMICAL BENCHMARK SYSTEM

Parameter	Value	Unit	Parameter	Value	Unit
ρ	0.15	kg/m ³	A2	3	m
kv_1, kv_2	0.5	kg/m s	x_{A0}	1	wt%
k_A	0.336	1/s	k_B	0.089	1/s
E_A/R	-100	kJ/kg	E_B/R	-150	kJ/kg
ΔH_A	-40	kJ/kg	ΔH_B	-50	kJ/kg
C_p	2.5	kJ/kg K	T_0	313	K

respectively. For simplicity, only the dynamics of the second reactor ($i = 2$) are herein considered, by assuming that its inputs (partially coinciding with the outputs of reactor 1) are independent terms. The nonlinear model of reactor 2 is

$$\begin{aligned}
 \dot{H}_2 &= \frac{1}{\rho A_2} (F_{20} + F_1 - F_2) \\
 \dot{x}_{A2} &= \frac{1}{\rho A_2 H_2} (F_{20} x_{A0} + F_1 x_{A1} - F_2 x_{A2}) - k_{A2} x_{A2}, \\
 \dot{x}_{B2} &= \frac{1}{\rho A_2 H_2} (F_1 x_{B1} - F_2 x_{B2}) + k_{A2} x_{A2} - k_{B2} x_{B2}, \\
 \dot{T}_2 &= \frac{1}{\rho A_2 H_2} (F_{20} T_0 + F_1 T_1 - F_2 T_2) \\
 &\quad - \frac{1}{C_p} (K_{A2} x_{A2} \Delta H_A + k_{B2} x_{B2} \Delta H_B) + \frac{Q_2}{\rho A_2 C_p H_2},
 \end{aligned} \tag{16}$$

where

$$\begin{aligned}
 F_i &= k_{vi} H_i \quad i \in \{1, 2\}, \\
 k_{A2} &= k_A \exp\left(-\frac{E_A}{RT_2}\right), \quad k_{B2} = k_B \exp\left(-\frac{E_B}{RT_2}\right).
 \end{aligned}$$

For the considered system, the output vector $y \in \mathbb{R}^4$ coincides with the state vector $x \in \mathbb{R}^4$, and the input vector $u \in \mathbb{R}^6$ are

$$\begin{aligned}
 y &= [H_2 \quad x_{A2} \quad x_{B2} \quad T_2]^T, \\
 u &= [H_1 \quad x_{A1} \quad x_{B1} \quad T_1 \quad F_{20} \quad Q_2]^T,
 \end{aligned}$$

where Q_2 is the external heating, F_{20} is the input flow of product A, and H_1, x_{A1}, x_{B1} and T_1 are the states associated to the first reactor. The values and units of the parameters of the benchmark system are collected in Table I. For a more detailed description of the system the interested reader is addressed to [40].

B. Training of an LSTM model of the system

An LSTM network is used to learn the chemical system in nominal conditions. To this end, following the guidelines described in [32] a single-layer LSTM network with 10 neurons and a linear output transformation has been adopted, with the structure depicted in Figure 2. A total of 136 input-output sequences has been collected from the simulated system (16), with sampling time $\tau = 0.1s$ and length $T_s = 100s$. Of these sequences, 100 have been used to train the LSTM network by minimizing the Mean Squared Error (MSE) between the collected outputs and the open-loop network's prediction, as discussed in [32]. The remaining 36 sequences have been used to independently test the LSTM model's performances. In Figures 3 and 4 the LSTM model's open-loop prediction

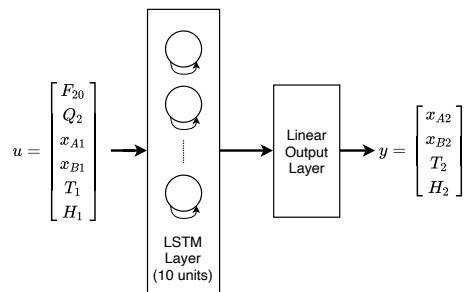


Fig. 2. Structure of one-layer LSTM network.

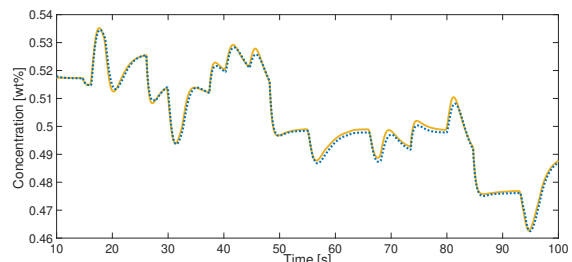


Fig. 3. Open-loop prediction of output x_{A2} by the LSTM model (blue dotted line) compared to the ground truth (yellow solid line).

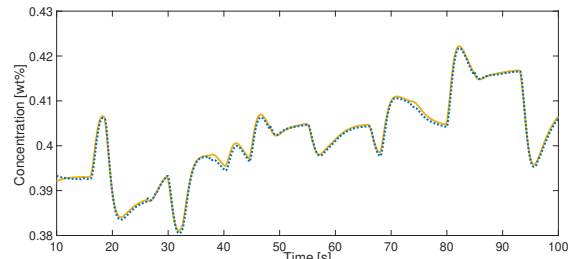


Fig. 4. Open-loop prediction of output x_{B2} by the LSTM model (blue dotted line) compared to the ground truth (yellow solid line).

of the outputs x_{A2} and x_{B2} are compared to the real output trajectories, respectively, for one of the test sequences. Note that the first 10 seconds of prediction are discarded, as they constitute the so-called washout period [32].

C. Parameter drift

In practice, a common phenomenon is that, during the operation of the plant, the value of some constant parameter varies for different reasons. For example, we consider the case where the parameter k_A drifts from value $k_A = 0.336$ to value $k_A = 0.326$ in the time interval $t \in [100, 200]$, as shown in Figure 5. Note that one may also consider the case where multiple parameters of the system change at the same time. The performance degradation of the LSTM model due to the occurrence of the drift is measured by collecting other 35 input-output sequences from the plant, and computing the MSE between the drifted system's output and the open-loop prediction of the model. The results, reported in Table II, witness a significant performance degradation. In particular, the MSE increases from $1.43 \cdot 10^{-5}$ to $31.48 \cdot 10^{-5}$, due to a degradation of outputs x_{A2} and x_{B2} modeling performances.

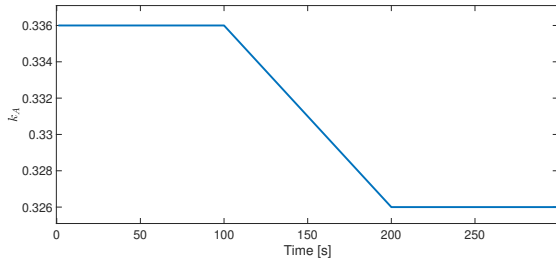


Fig. 5. Drift of parameter k_A .

TABLE II
MODELING PERFORMANCES OF THE UNADAPTED LSTM

Scenario	H_2	MSE [$\cdot 10^{-5}$]			Average
		x_{A2}	x_{B2}	T_2	
before drift	0.78	1.36	1.06	2.53	1.43
after drift	0.77	46.74	77.16	2.72	31.84

D. MHE for LSTM parameter tuning

To mitigate for the impact of the parameter drift on the modeling performances, the LSTM model needs to be tuned on-line. To this end, we implemented the algorithm proposed in Section II where, since the network state is not measured, a state observer has been used [32]. Hence, during the parameter drift the LSTM weights have been tuned by means of the MHE algorithm. The nonlinear optimization problem (2) consists of 724 optimization variables, i.e. the network's weights, and it has been solved with MATLAB's *fmincon*.

Different values of the MHE hyperparameters μ and N have been tested, validating the modeling performances of the resulting (tuned) LSTM model on the same 35 sequences on which, in Section III-C, the performance degradation of the nominal LSTM model has been assessed.

In Table III the computational burden and the simulation error achieved by the tuned LSTM models are reported, witnessing a remarkable reduction of the MSE compared to that scored by the nominal (unadapted) LSTM model (see Table II). In particular, the best performances are achieved selecting $\mu = 0.1$ and $N = 10$, that allow to reduce the MSE from $31.84 \cdot 10^{-5}$ to $7.24 \cdot 10^{-5}$, i.e. a 77% reduction. The corresponding open-loop prediction of x_{A2} and x_{B2} are reported in Figure 6 and Figure 7.

TABLE III
MHE PARAMETERS AND TUNED LSTM'S MODELING PERFORMANCES

Parameters		Comp. time [s]	MSE [$\cdot 10^{-5}$]				Average
μ	N		H_2	x_{A2}	x_{B2}	T_2	
0.05	10	33.6	2.19	9.01	14.28	3.99	7.37
0.1	5	13.7	2.32	8.62	15.33	6.89	8.29
0.1	10	24.8	1.81	9.33	13.6	4.26	7.24
0.1	20	39.6	3.23	8.09	19.55	8.00	9.72
0.5	10	17.45	1.99	8.79	16.28	6.69	8.44

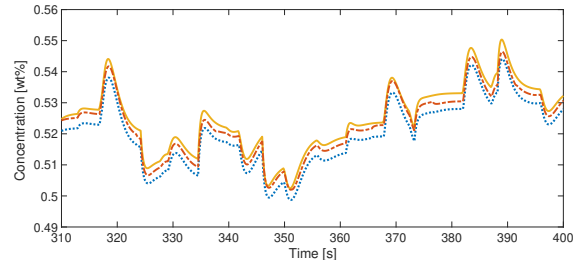


Fig. 6. Open-loop prediction of x_{A2} by the unadapted LSTM model (blue dotted line) and tuned LSTM model (red dashed line) compared to the ground truth (yellow solid line), with $\mu = 0.1$ and $N = 10$.

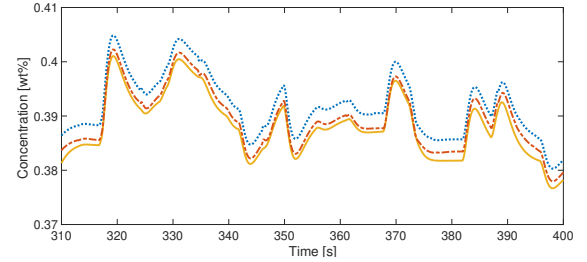


Fig. 7. Open-loop prediction of x_{B2} by the unadapted LSTM model (blue dotted line) and tuned LSTM model (red dashed line) compared to the ground truth (yellow solid line), with $\mu = 0.1$ and $N = 10$.

IV. CONCLUSIONS AND FUTURE DIRECTIONS

In this paper, a possible solution to the lifelong learning problem for RNNs used as dynamic systems models is presented. The theoretical convergence properties of the proposed method, which is based on a Moving Horizon Estimation strategy, have been analyzed, and its performances have been evaluated on a nontrivial simulated chemical plant, already widely used as benchmark in the control community.

Notably, although it is assumed that no measurement noise affects the system, white gaussian noise could be easily included while preserving the boundedness of the weight estimation error.

While promising results have been achieved, there are many open questions that need to be investigated and that may draw future research directions. First and foremost, the state is herein assumed to be known. While this is true when NNARX are used, this is not the case for other RNN architectures, which instead call for the design of a suitable state observer. Albeit, from a theoretical point of view, one could simply extend the state equations with fictitious dynamics of the parameters [36], [42], [43], this approach could lead to an intractable optimization problem. A possible solution towards this issue would exist if the state estimation is unconstrained, and it would consist of a combination of the proposed method with a Luenberger observer.

A second problem concerns the scalability of the optimization problem here proposed. Indeed, Neural Networks are generally characterized by a possibly large number of weights. For non-small NNs, this may lead to a large computational burden, or even intractability, although relieving strategies, such as batch operation, could be adopted.

ACKNOWLEDGMENTS



This project has received funding from the European Union's Horizon 2020 research and innovation programme under the Marie Skłodowska-Curie grant agreement No. 953348

REFERENCES

- [1] A. Cossu, A. Carta, V. Lomonaco, and D. Bacciu, "Continual learning for recurrent neural networks: An empirical evaluation," *Neural Networks*, vol. 143, pp. 607–627, 2021.
- [2] V. Losing, B. Hammer, and H. Wersing, "Incremental on-line learning: A review and comparison of state of the art algorithms," *Neurocomputing*, vol. 275, pp. 1261–1274, 2018.
- [3] G. I. Parisi, R. Kemker, J. L. Part, C. Kanan, and S. Wermter, "Continual lifelong learning with neural networks: A review," *Neural Networks*, vol. 113, pp. 54–71, 2019.
- [4] S. Sodhani, S. Chandar, and Y. Bengio, "Toward training recurrent neural networks for lifelong learning," *Neural computation*, vol. 32, no. 1, pp. 1–35, 2020.
- [5] Y. Wu, Y. Chen, L. Wang, Y. Ye, Z. Liu, Y. Guo, and Y. Fu, "Large scale incremental learning," in *Proceedings of the IEEE/CVF Conference on Computer Vision and Pattern Recognition*, 2019, pp. 374–382.
- [6] G. M. Van de Ven and A. S. Tolias, "Three scenarios for continual learning," *arXiv preprint arXiv:1904.07734*, 2019.
- [7] T. Mitchell, W. Cohen, E. Hruschka, P. Talukdar, B. Yang, J. Beteridge, A. Carlson, B. Dalvi, M. Gardner, B. Kisiel *et al.*, "Never-ending learning," *Communications of the ACM*, vol. 61, no. 5, pp. 103–115, 2018.
- [8] A. U. Levin and K. S. Narendra, "Control of nonlinear dynamical systems using neural networks: Controllability and stabilization," *IEEE Transactions on neural networks*, vol. 4, no. 2, pp. 192–206, 1993.
- [9] —, "Identification using feedforward networks," *Neural Computation*, vol. 7, no. 2, pp. 349–369, 1995.
- [10] P. Sastry, G. Santharam, and K. Unnikrishnan, "Memory neuron networks for identification and control of dynamical systems," *IEEE transactions on neural networks*, vol. 5, no. 2, pp. 306–319, 1994.
- [11] J. M. Ali, M. A. Hussain, M. O. Tade, and J. Zhang, "Artificial intelligence techniques applied as estimator in chemical process systems—a literature survey," *Expert Systems with Applications*, vol. 42, no. 14, pp. 5915–5931, 2015.
- [12] D. M. Himmelblau, "Accounts of experiences in the application of artificial neural networks in chemical engineering," *Industrial & Engineering Chemistry Research*, vol. 47, no. 16, pp. 5782–5796, 2008.
- [13] S. Piche, B. Sayyar-Rodsari, D. Johnson, and M. Gerules, "Nonlinear model predictive control using neural networks," *IEEE Control Systems Magazine*, vol. 20, no. 3, pp. 53–62, 2000.
- [14] M. A. Hosen, M. A. Hussain, and F. S. Mjalli, "Control of polystyrene batch reactors using neural network based model predictive control (nnmpc): An experimental investigation," *Control Engineering Practice*, vol. 19, no. 5, pp. 454–467, 2011.
- [15] Z. K. Nagy, "Model based control of a yeast fermentation bioreactor using optimally designed artificial neural networks," *Chemical engineering journal*, vol. 127, no. 1–3, pp. 95–109, 2007.
- [16] H. Jaeger, "The "echo state" approach to analysing and training recurrent neural networks—with an erratum note," *Bonn, Germany: German National Research Center for Information Technology GMD Technical Report*, vol. 148, no. 34, p. 13, 2001.
- [17] Y. Pan and J. Wang, "Model predictive control of unknown nonlinear dynamical systems based on recurrent neural networks," *IEEE Transactions on Industrial Electronics*, vol. 59, no. 8, pp. 3089–3101, 2011.
- [18] P. G. Plöger, A. Arghir, T. Günther, and R. Hosseiny, "Echo state networks for mobile robot modeling and control," in *Robot Soccer World Cup*. Springer, 2003, pp. 157–168.
- [19] S. Hochreiter and J. Schmidhuber, "Long short-term memory," *Neural computation*, vol. 9, no. 8, pp. 1735–1780, 1997.
- [20] Z. Wu, A. Tran, D. Rincon, and P. D. Christofides, "Machine learning-based predictive control of nonlinear processes. part i: Theory," *AIChE Journal*, vol. 65, no. 11, 2019.
- [21] N. Mohajerin and S. L. Waslander, "Multistep prediction of dynamic systems with recurrent neural networks," *IEEE transactions on neural networks and learning systems*, vol. 30, no. 11, pp. 3370–3383, 2019.
- [22] A. Rehmer and A. Kroll, "On using gated recurrent units for nonlinear system identification," in *2019 18th European Control Conference (ECC)*. IEEE, 2019, pp. 2504–2509.
- [23] F. M. Bianchi, E. Maiorino, M. C. Kampffmeyer, A. Rizzi, and R. Jenssen, *Recurrent neural networks for short-term load forecasting: an overview and comparative analysis*. Springer, 2017.
- [24] E. D. Sontag and Y. Wang, "On characterizations of the input-to-state stability property," *Systems & Control Letters*, vol. 24, no. 5, pp. 351–359, 1995.
- [25] Z.-P. Jiang and Y. Wang, "Input-to-state stability for discrete-time nonlinear systems," *Automatica*, vol. 37, no. 6, pp. 857–869, 2001.
- [26] D. Angeli, "Further results on incremental input-to-state stability," *IEEE Transactions on Automatic Control*, vol. 54, no. 6, pp. 1386–1391, 2009.
- [27] F. Bayer, M. Bürger, and F. Allgöwer, "Discrete-time incremental iss: A framework for robust nmpc," in *2013 European Control Conference (ECC)*. IEEE, 2013, pp. 2068–2073.
- [28] F. Bonassi, M. Farina, and R. Scattolini, "Stability of discrete-time feed-forward neural networks in NARX configuration," in *19th IFAC Symposium on System Identification (SYSID 2021)*, 2021.
- [29] L. B. Armenio, E. Terzi, M. Farina, and R. Scattolini, "Model predictive control design for dynamical systems learned by echo state networks," *IEEE Control Systems Letters*, vol. 3, no. 4, pp. 1044–1049, 2019.
- [30] F. Bonassi, E. Terzi, M. Farina, and R. Scattolini, "LSTM neural networks: Input to state stability and probabilistic safety verification," in *Learning for Dynamics and Control*. PMLR, 2020, pp. 85–94.
- [31] F. Bonassi, M. Farina, and R. Scattolini, "On the stability properties of gated recurrent units neural networks," *Systems & Control Letters*, vol. 157, p. 105049, 2021.
- [32] E. Terzi, F. Bonassi, M. Farina, and R. Scattolini, "Learning model predictive control with long short-term memory networks," *International Journal of Robust and Nonlinear Control*, 2021.
- [33] F. Bonassi, C. F. Oliveira da Silva, and R. Scattolini, "Nonlinear MPC for offset-free tracking of systems learned by GRU neural networks," in *3rd IFAC Conference on Modelling, Identification and Control of Nonlinear Systems (MICNON)*, vol. 54, no. 14, 2021, pp. 54–59.
- [34] C. V. Rao, J. B. Rawlings, and J. H. Lee, "Constrained linear state estimation—a moving horizon approach," *Automatica*, vol. 37, no. 10, pp. 1619–1628, 2001.
- [35] J. Rawlings and D. Mayne, *Model predictive control: theory and design*. Nob Hill Publishing, 2009.
- [36] A. Alessandri, M. Baglietto, and G. Battistelli, "Moving-horizon state estimation for nonlinear discrete-time systems: New stability results and approximation schemes," *Automatica*, vol. 44, no. 7, pp. 1753–1765, 2008.
- [37] A. Cossu, A. Carta, and D. Bacciu, "Continual learning with gated incremental memories for sequential data processing," in *2020 International Joint Conference on Neural Networks (IJCNN)*. IEEE, 2020, pp. 1–8.
- [38] X. Guo *et al.*, "Continual learning long short term memory," in *Proceedings of the 2020 Conference on Empirical Methods in Natural Language Processing: Findings*, 2020, pp. 1817–1822.
- [39] M. Mercangöz, A. Cortinovis, and S. Schönborn, "Autonomous process model identification using recurrent neural networks and hyperparameter optimization," *IFAC-PapersOnLine*, vol. 53, no. 2, pp. 11 614–11 619, 2020.
- [40] B. T. Stewart, A. N. Venkat, J. B. Rawlings, S. J. Wright, and G. Pannocchia, "Cooperative distributed model predictive control," *Systems & Control Letters*, vol. 59, no. 8, pp. 460–469, 2010.
- [41] P. Kumar, J. B. Rawlings, and S. J. Wright, "Industrial, large-scale model predictive control with structured neural networks," *Computers & Chemical Engineering*, vol. 150, p. 107291, 2021.
- [42] P. Kühl, M. Diehl, T. Kraus, J. P. Schöder, and H. G. Bock, "A real-time algorithm for moving horizon state and parameter estimation," *Computers & chemical engineering*, vol. 35, no. 1, pp. 71–83, 2011.
- [43] D. G. Robertson, J. H. Lee, and J. B. Rawlings, "A moving horizon-based approach for least-squares estimation," *AIChE Journal*, vol. 42, no. 8, pp. 2209–2224, 1996.